# Supporting Information

## *Individual Concave Twin ZnO Microdisk with optical resonance*

Yumin Chen, *[a, b, c, d] Zhen Liu,[b] Xiaohui Qiu[b, d] and Xinfeng Liu*[b, d]

*a. State Key Laboratory of Structural Chemistry, Fujian Institute of Research on the Structure of Matter, Chinese Academy of Sciences, Fuzhou 350002, China*
*b. CAS Key Laboratory of Standardization and Measurement for Nanotechnology, CAS Center for Excellence in Nanoscience, National Center for Nanoscience and Technology; Beijing 100190, P. R. China.*
*c. Center for Excellence in Regional Atmospheric Environment, Key Laboratory of Urban Pollutant Conversion, Institute of Urban Environment, Chinese Academy of Sciences, Xiamen 361021, China*
*d. University of Chinese Academy of Sciences, Beijing 100049, P. R. China.*

## Experimental details

### Chemical synthesis

Zinc acetate dehydrate (98%), sulfur (powder, 99.98%) and dodecyl amine (98%) were purchased from Aldrich. Ethanol, hexane and carbon disulfide were purchased from Sinopharm Chemical Reagent Co. Ltd. All chemicals were used without further purification. Dodecyl amine was melted in advance at 60℃ if it freezes into solid.

The fabrication of concave ZnO microdisks was realized by a solvothermal reaction using dodecyl amine as solvent and structure-directing agent, zinc acetate dehydrate as Zn source, sulfur as promoter. 4 mmol zinc acetate dehydrate was mixed with 10 ml melting dodecyl amine and then heated at 60℃ for 0.5 h under stirring. 0-4 mmol sulfur powder was further added into the mixture, heated at 60℃ and stirred for about 2 min till the mixture turned into olive green transparent liquid. The mixture was transferred into a 20 ml Teflon-line stainless-steel autoclave and put into a 120℃ oven. After heated for 1h, the reactor was transferred to another 220℃ oven and further heated for several hours as desired before terminating the reactions.

After the reaction, the precipitates which are our target product (concave ZnO microdisks) were separated through the filtration and emphatically investigated in this work. The precipitates were ultrasonic cleaned by ethanol and carbon disulfide alternately for three times and then dispersed in hexane. The upper ZnS colloids were also collected, centrifuged and washed by ethanol for several times and then dispersed in ethanol.

### Structure characterization

The morphology of the as-prepared precipitated products (concave ZnO microdisks) was investigated by scanning electron microscopy (SEM, Hitachi 4800 or Hitachi SU8010 or FEI phenom G2). The SEM sample was prepared by depositing a drop of suspension of ZnO precipitant onto the clean silicon surface. By rotating SEM sample stage, the morphologies of ZnO can be observed from various viewing angles. The crystal structure was acquired by transmission electron microscopy (TEM, FEI-F20) with an acceleration voltage of 200 kV. The TEM sample was prepared by depositing a drop of suspension of ZnO precipitant or ZnS colloids onto the carbon coated copper grid. Energy Dispersive Spectrometer (EDS) which was equipped in SEM gave out the chemical composition of samples at the same time. The crystal phase was characterized by powder X-ray diffractometer (XRD, Rigaku Miniflex Ⅱ) with a Cu KR radiation source.

### Optical measurement

The sample was prepared through high-speed spin coating a drop of ZnO suspension in ethanol onto a silicon wafer and then drying in an vacuum oven at 80℃ for 8h. For optical measurements of individual concave ZnO microdisks, high-speed spin ensures the particle spacing far enough and no interactions between each other. Photoluminescence (PL) measurements were performed by a commercial confocal Raman microscope (Horiba Jobin Yvon LabRAM, France) using a He-Cd laser (10 mW output) with a wavelength of 325 nm as the excitation source. The laser was focused onto individual ZnO microdisks with a 20 μm diameter light spot. All experiments were carried out at room temperature.

## Supported data and discussion

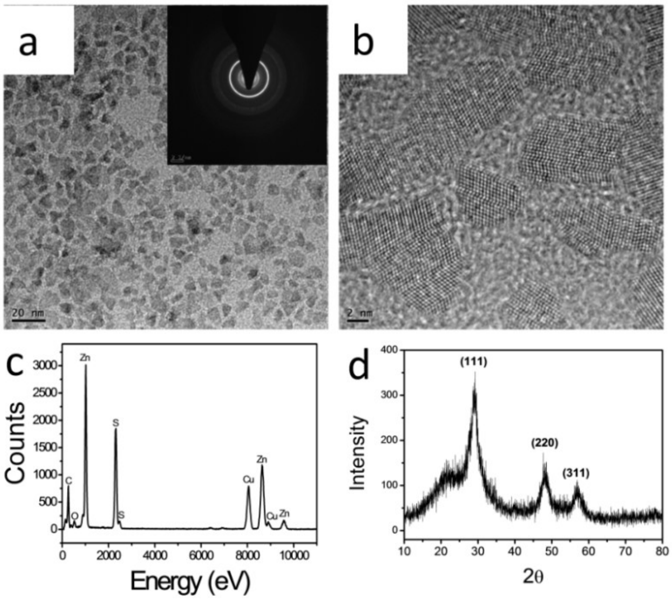

**Figure S1** Structure and composite characterization of the upper ZnS colloid products. (a) A large-scale TEM image of ZnS nanoparticles. SAED is inserted in the top right corner. (b) HRTEM image of ZnS nanoparticles. (c) EDS spectroscopy of ZnS nanoparticles which confirms the chemical composition. (d) XRD pattern of ZnS nanoparticles which indicates they are cubic sphalerite.

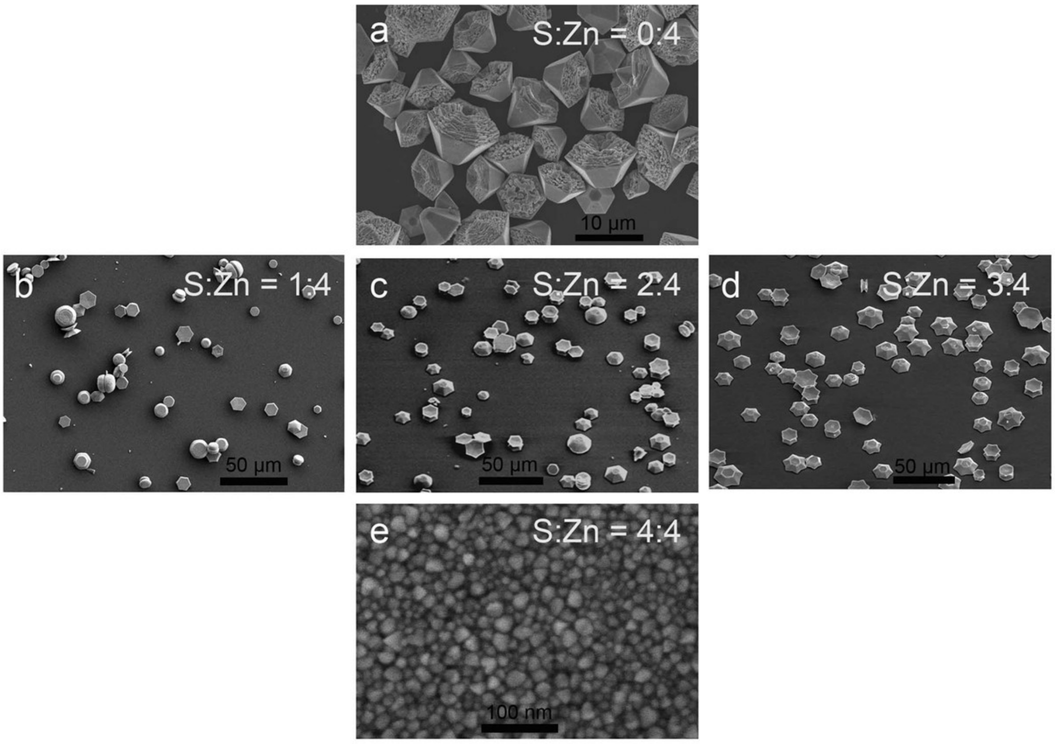

**Figure S2** (a-d) SEM images of the precipitate ZnO products prepared at S/Zn ratio of 0:4, 1:4, 2:4 and 3:4. Since we concerned the structure evolution of ZnO microdisks, so the upper colloid products were removed in advance and haven’t displayed here. (e) SEM image of ZnS colloids prepared at S/Zn ratio of 4:4. Since ZnS colloids are the only product, so no micron sized ZnO particles was shown at this preparation condition. All products were prepared at 120℃ for 1h and then 220℃ for 9h.

A series of control experiments reveals that an appropriate S/Zn ratio is very important for the formation of the concave ZnO microdisks (Figure S2). If the S/Zn ratio is 0/4 or 4/4, only ZnO hierarchical structure or ZnS nanoparticles come into being and no concave microdisks emerge. When the S/Zn ratio is controlled at a suitable value (such as 1/4, 2/4 or 3/4), concave microdisks will form under the circumstance that mutual products (ZnS and ZnO) coexist. S/Zn ratio is not only a critical factor to decide whether the concave microdisks form, but also affect their fine structures and morphologies. In a word, it is very crucial to bringing in a competitive reaction to produce ZnS nanoparticles for the formation of concave twin ZnO microdisks.

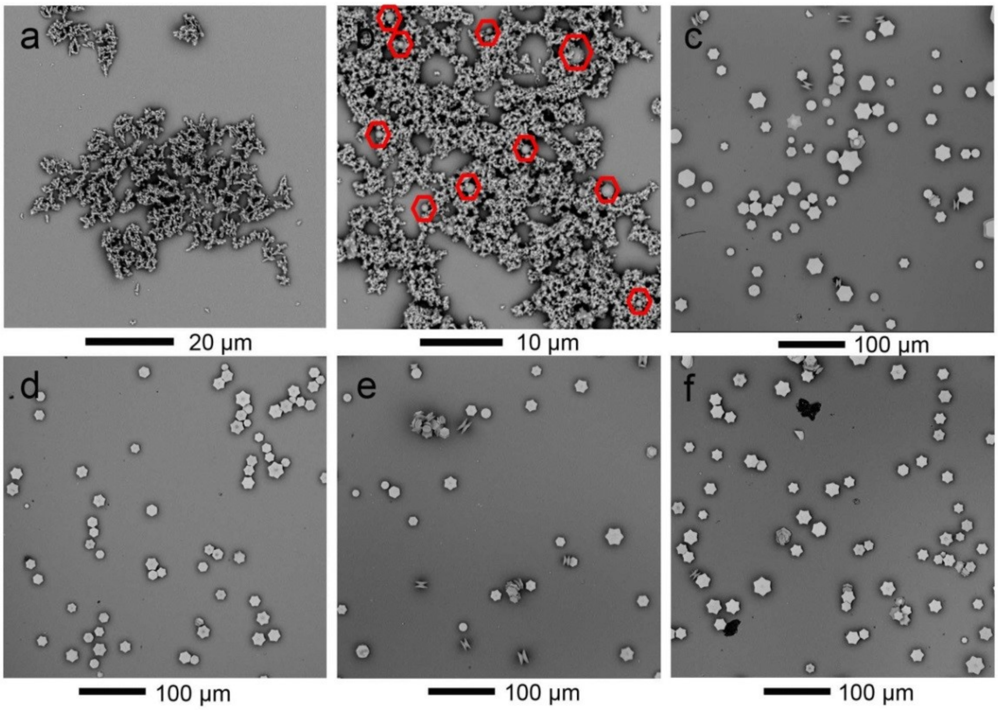

**Figure S3** SEM images of main products after the reactions were performed at 120℃ for 1h and then 220℃ for xh. (a) x = 0; (b) x = 0.5h; (c) x = 1h; (d) x = 1.5h; (e) x = 2h; (f) x = 3h. All products were prepared at the S/Zn ratio of 3:4. Since we concerned the morphology evolution of microdisks, we paid attention on the morphologies of the precipitate products. In the cases from (c) to (f), the upper colloid products have been separated from the precipitated products and have not been shown in SEM images. But in the early nucleation stages, only nanoparticles come into being, so we observed the morphologies of all products (Figures a and b).

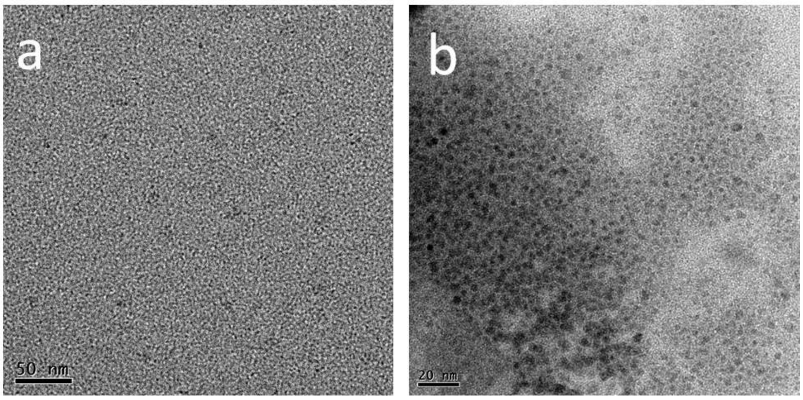

**Figure S4** TEM images of products after the reactions were performed at 120℃ for 1h and then 220℃ for xh. (a) x = 0; (b) x = 0.5h. All products were prepared at the S/Zn ratio of 3:4.

A series of time-dependent control experiments were performed at 120℃ for 1h and then continued to go on at 220℃ for x hours (x = 0, 0.5, 1, 1.5, 2 and 3h) (see Figure S3 & Figure S4). Nanoparticle colloids come into being at the nucleation stage when the reaction was carried out at 120℃ for 1h (Figure S3a & Figure S4a). And then a small amount of ZnO nanoparticles with several hundred nanometers (marked by circles in Figure S3b) appear with a large number of nanoparticle (Figure S4b) when the reaction continued at 220℃ for 0.5h. When the reactants continued to be heated at 220℃ for 1h, 1.5h, 2h and 3h, concave ZnO microdisks were produced in the form of precipitation coexisted with the upper ZnS nanoparticle colloids, which have been washed away and not shown here (Figures S3c-f). Two competitive reactions coexist; as a result, the growth dynamic of ZnO microdisks is tuned by the reaction of producing ZnS nanoparticles.

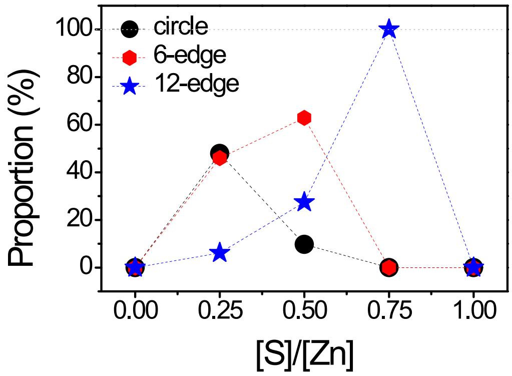

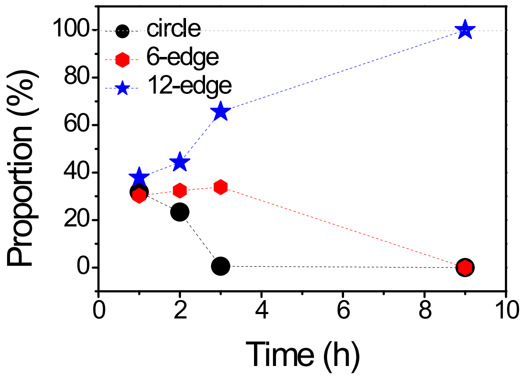

**Figure S5** (a) morphology statistics of ZnO microdisks with the various [S]/[Zn] ratios. (b) Morphology statistics of ZnO microdisks with the reaction time in the growth process.

Careful observation reveals that the cross section of the concave ZnO microdisks may be round, hexagonal or dodecagonal, and their quantity percentages change with the increase of S/Zn ratio or reaction time. Statistical analysis results (Figure S5) show that the morphology evolution from round to hexagonal and then to dodecagonal microdisks is pushed forwards by increasing the S/Zn ratio or reaction time. Large S/Zn ratio or reaction time promotes the improvement of concavity of microdisks. As Figure S6 shown, nearly all ZnO microdisks can be controlled to dodecagonal plates through adjusting the S/Zn ratio and reaction time.

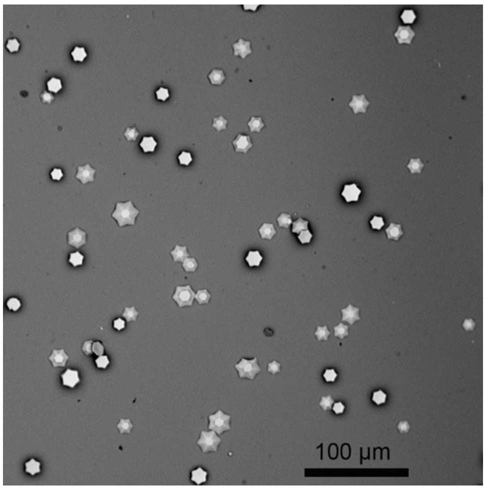

**Figure S6** A large-scale SEM image of twin concave dodecagonal ZnO microdisks. Nearly all microdisks are dodecagonal and no hexagonal and ground microdisks coexist.

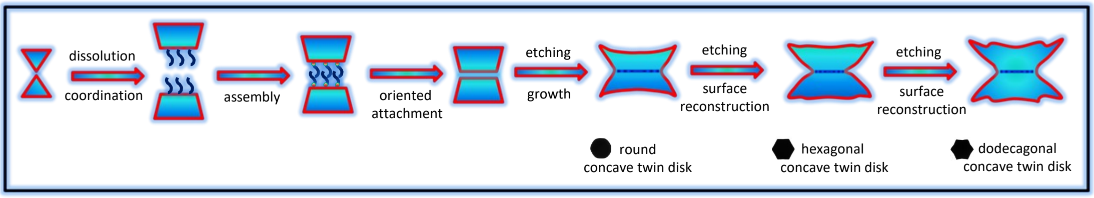

**Figure S7** A possible growth process schematic diagram of twin concave ZnO microdisks.

A schematic diagram for the possible growth process of concave twin ZnO microdisks was proposed (Figure S7). When S powder was added and the reactants were heated to 120℃ at the hydrothermal reactor, a large number of ZnS nanoparticles rapidly form in the supersaturated state. Excessive $Zn^{2+}$ form ZnO hexagonal pyramid seed at the alkaline conditions when the reaction temperature was further elevated to 220℃. The spires of hexagonal pyramids are easily dissolved and hexagonal prismoids form. Nevertheless, the $Zn^{2+}$ (0001) surface bonds strongly to dodecyl amine due to the coordination and the densely packed dodecyl amine protect the surface from further growth or etching along [0001] direction, resulting in the formation of the flat side of the microdisks.[1] To reduce the interfacial energy, two hexagonal prismoids oriented attach along the [0001] direction, with the help of the van der Waals interactions between the long tails of the self-assembled dodecyl amine monolayer adsorbed on the two flat (0001) surfaces.[2] Initial nucleation acts as a twin microdisk boundary, and then the incoming atoms adsorbed on the two sides to form a symmetric twin structure.[3] Two paired disks with the nearly same size are symmetrically distributed, suggesting that the twin structure may form via oriented attachment in the early growth period. In addition, a few of single disks may coexist with twin disks after the ultrasonic treatment, which confirms that the binding forces between two paired disks are a little weak in the oriented attachment mechanism. At the growth stage, ZnO will dissolute along the c axis simultaneously in a high concentration alkaline solution and etching is preferential to happen at the center of the exposed $O^{2-}$(000-1) surface, resulting in a concave surface.[1, 4] Etching leads to rough and uneven concave surfaces are uneven in the initial time. Based on the results of our control experiments (Figure S2 to Figure S5), we deduced that surface reconstruction and further growth driven by the co-existence of the two competitive reactions to form ZnO or ZnS is the possible reason to explain the formation of well-defined concave structure with high-energy facets.

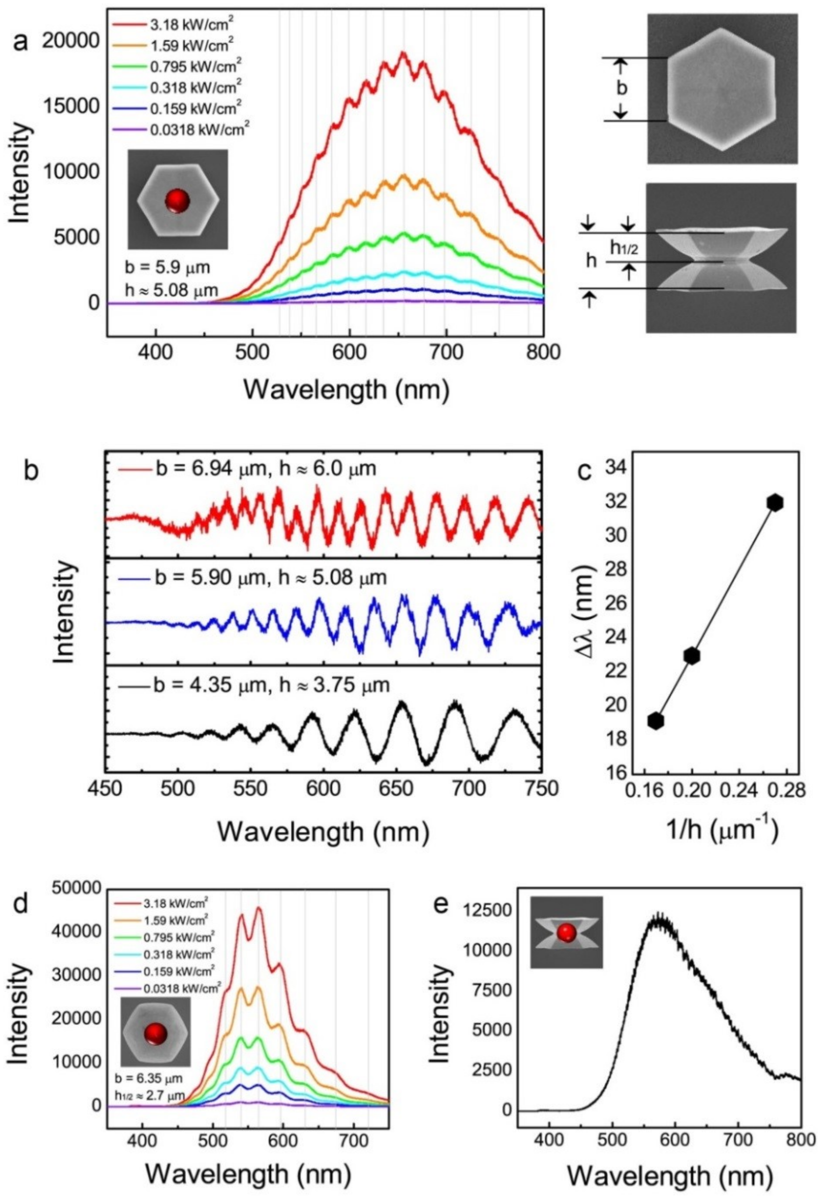

**Figure S8** Photoluminescence (PL) spectrums of individual hexagonal concave ZnO microdisks at room temperature. (a) Pump density dependent PL spectrums of hexagonal concave twin microdisks (light irradiation parallel to the [0001] direction of microdisks). The center position of incident exciting laser projection was marked by a red ball. (b) Size dependent PL spectrums of hexagonal concave twin microdisks. The incident exciting light was irradiated parallel to the [0001] direction and focus on the center of the microdisks. (c) The relationship between $\Delta\lambda$ and 1/h derived from Figure S4b. (d) Pump density dependent PL spectrums of hexagonal concave single-microdisks (the incident light is parallel to the [0001] direction from the back side of the single-microdisk). The center position of incident exciting laser projection was marked by a red ball. (e) PL spectrum of hexagonal concave twin microdisks (the light irradiation direction is perpendicular to the [0001] direction). The center position of the incident exciting laser projection was marked by a red ball. Note: the values of the edge length (b) and height of concave hexagonal ZnO microdisks (h and $h_{1/2}$) were shown near their corresponding PL spectrums.

## Reference

(1) F. Li, Y. Ding, P. Gao, X. Xin and Z. Wang, Angew. Chem. Int. Ed. 2004, 43, 5238.
(2) T. Zhang, W. Dong, M. K.-B., S. K., R. N. N. and Z. R. Tian, JACS, 2006, 128: 10960.
(3) C. Xu, X. W. Sun, Z. L. Dong, Y. P. Cui and B. P. Wang, Cryst. Growth Des. 2007, 7: 541.
(4) X. Hang, X. Zhou, Y. Jiang and Z. Xie, Jour. Mat. Chem. 2012, 22: 10924.